International Journal of Lightweight Materials and Manufacture 4 (2021) 62–66

Contents lists available at ScienceDirect

International Journal of Lightweight Materials and Manufacture

journal homepage: https://www.sciencedirect.com/journal/international-journal-of-lightweight-materials-and-manufacture

Original Article

Al foams manufactured by PLA replication and sacrifice

Girolamo Costanza [a, *], Maria Elisa Tata [b], Giuseppe Trillicoso [a]

[a] Industrial Engineering Department, University of Rome Tor Vergata, Via del Politecnico, 1- 00133, Rome, Italy
[b] Computer Science and Civil Engineering Department, University of Rome Tor Vergata, Via del Politecnico, 1- 00133, Rome, Italy

ARTICLE INFO

Article history:
Received 1 May 2020
Received in revised form
8 July 2020
Accepted 9 July 2020
Available online 18 July 2020

Keywords:
Metal foam
3D printing
PLA
Elementary cell
Truncated octahedron

ABSTRACT

A new method for the manufacturing of pre-determined open porosity Al foams is presented in this work. Starting from a 3D foam model designed with CAD and printed with fused deposition modeling (FDM), a porous structure of poly lactic acid (PLA) has been replicated. The choice of this material has been driven by the properties in terms of recyclability and low cost. The truncated octahedron for the porosity shape has been selected due to benefit and properties ascribable to its morphology. After creating the 3D PLA model, it has been filled with liquid plaster. After its solidification, PLA is removed in oven at 600 °C so that a negative-shaped plaster mold is obtained. Successively liquid Al at 750 °C is poured in the mold inside the oven. After Al solidification, plaster can be easily removed in ultrasonic bath thus obtaining Al foam with the same morphology of the starting PLA model. This process shows great flexibility allowing to manufacture different kind of elementary cell types. Tailoring of the selected properties of the manufactured foams, e.g. the morphology, the density or the surface/volume ratio may be obtained. With this technique many other metals and alloys can be manufactured too. The potential of this production technique can be successfully employed in many application fields of metal foam. Lightweight 3D lattice structures are widely employed for multifunctional applications such as loading bearing, negative and zero thermal-expansion structures, vibration attenuation, impact and blast proof structures.

1. Introduction

Cellular materials are made of interconnected lines or surfaces network of various thickness to form the so called “elementary cells”. These cells can be polyhedral or spherical and the mechanical and physical properties of the cellular solids depend directly on the shape, size and distribution of the elementary cells. Porous structures are also widespread in nature: some examples are wood, cork, tuff, sponge, coral, bones and bee's honeycomb. Natural cellular materials are widely employed nowadays for thermal and sound insulation as well for lightweight construction [1]. Synthetic cellular materials (polymeric, ceramic and metallic) can easily substitute natural ones, with the further advantage that in many cases the porosity size and shape can be selected a priori. A morphological classification of cellular solids can be made as follows: two-dimensional cells (in which the cell walls have a common generator as in honeycomb structure) and three-dimensional cellular solid (usually called foams) [2]. Dealing with foams they can be classified according to the morphology of the cavities that can be separated each other (closed cell foam) or interconnected (open cell foam). This feature deeply influences the foam properties and consequently their potentialities. In many applications, for instance, it is required that a medium (liquid or gas) flows through the foams; in this case various degrees of open cell foams may be employed. On the other hands for structural applications, in which metal foams are able to absorb energy during the deformation, a completely closed cell structure is necessary. Another classification can be made according to the application field: in the “functional” one (heat exchangers, filters, catalyst supports, silencers) metal foams play a functional role while in the “structural” one (energy absorbers, load-bearing components) the foams are subjected to an external load. More in general the properties of metal foams depend on: metallurgy (metal or alloys they are made of), processing morphology (type of porosity open or closed), amount of porosity, cell size and shape.

In the last twenty years the researcher's attention has been focused on cellular foams more in general [3] and metal foams in

* Corresponding author.
E-mail address: costanza@ing.uniroma2.it (G. Costanza).
Peer review under responsibility of Editorial Board of International Journal of Lightweight Materials and Manufacture.

https://doi.org/10.1016/j.ijlmm.2020.07.001

particular [4]. About the production methods, many techniques have been developed in order to manufacture foams. They can be classified according to the state of the processed metal: from metal vapor or gaseous metallic compounds (metal deposition on cellular preform), from liquid metal (melt gas injection, gas-releasing particle decomposition in the melt etc.); from solid metal in powdered form (hollow sphere structure, gas-releasing particle decomposition in semisolid, entrapped gas expansion etc.) [2]. Some studies have been aimed to the optimization of the powder mix composition and its effects on the foam morphology in closed-cell foams [5,6]. One of the most important structural features of cellular solids is the relative density (ρ^*/ρ_o) that is a ratio of the density of the foam to the density of the solid. The porosity can be ascribed to the fraction of pores in the cellular solids. Usually cellular solids have relative densities also lower than 0.3. Another important issue is the energy absorption during compaction and crushing. The porosity and the wall collapse during the deformation allow to obtain a stress-strain curve characterized by a wide plateau stress during which high strain occurs, as evidenced in some research papers [7–9].

Current research is focused on the built-up of a new foam production process, on the implementation of process control to produce more homogeneous materials and to achieve a better reproducibility and predictability of the morphological and mechanical properties. Both for functional and structural applications the uniformity of the porosity size, shape and inter-pore channel is extremely important. Cost reduction is another important task and can be achieved, for instance, by using cheaper material, by simplifying the processing steps or employing scraps instead of more expensive powders, as evidenced for the case of lead foams by Costanza et al. in Ref. [10].

This work aims to introduce an alternative method to obtain open cell foams with an excellent repeatability of the porosity size and shape but at the same time in a cheaper manner. The flexibility of the suggested process allows the selection of the kind of porosity depending on the application. Gibson and Ashby [11] analyzed the properties of cellular materials depending on the way the solid is distributed in the cell faces and edges. They described the topological laws governing the shape and the size of the cells and then equations relating density to the cell wall thickness and length for cellular solid have been developed. In the following lines correlation formulas between relative density and the different type of cells are reported for some examples of 3D open cells (aspect ratio A_r = h/l).

Triangular prisms

$$Z_e = 8,\ Z_f = 4.5,\ \overline{n} = 3.6,\ \overline{f} = 5 \qquad \frac{\rho^*}{\rho_s} = \frac{2}{\sqrt{3}}\frac{t^2}{l^2}\left(1 + \frac{3}{A_r}\right)$$

Square prisms

$$Z_e = 6,\ Z_f = 4,\ \overline{n} = 4,\ \overline{f} = 6 \qquad \frac{\rho^*}{\rho_s} = \frac{t^2}{l^2}\left(1 + \frac{2}{A_r}\right)$$

Hexagonal prisms

$$Z_e = 5,\ Z_f = 3.6,\ \overline{n} = 4.5,\ \overline{f} = 8 \qquad \frac{\rho^*}{\rho_s} = \frac{4}{3\sqrt{3}}\frac{t^2}{l^2}\left(1 + \frac{3}{2A_r}\right)$$

Rombic dodecahedra

$$Z_e = 5.33,\ Z_f = 3,\ \overline{n} = 4, \qquad \overline{f} = 12\frac{\rho^*}{\rho_s} = 2.87\frac{t^2}{l^2}$$

Tetrakaidecahedra

$$Z_e = 4,\ Z_f = 3,\ \overline{n} = 5.14, \qquad \overline{f} = 14\frac{\rho^*}{\rho_s} = 1.06\frac{t^2}{l^2}$$

where Z_e is the edge-coordination, Z_f is the face-coordination, n is the average number of edges, f is the average number of faces, t is the thickness and l the length of the edge, ρ^* is the density of the foam and ρ_s is the density of the solid.

The correlation between relative density and mechanical properties has been object of the researcher attention starting from the work of Gibson and Ashby [11,12]:

$$\left(\frac{E}{E_O}\right) = \left(\frac{\rho}{\rho_O}\right)^2$$

little adjustments have been introduced by the model of Murr et al. [13]:

$$\left(\frac{E}{E_O}\right) = \left(\frac{\rho}{\rho_O}\right)^{2.1}$$

and by the model of Cheng et al. [14]:

$$\left(\frac{E}{E_O}\right) = \left(\frac{\rho}{\rho_O}\right)^{2.4}$$

The differences in the mechanical behavior vs relative density between the three models for the rhombidodecahedron sandwich structure are well illustrated in Fig. 1.

The main goal of this paper is to suggest an alternative process to obtain open cell foams with pre-selected geometry of the cell, in a cheaper way and with high repeatability able to vary the cell size and shape according to the properties that are requested in the final application. Purely by way of example a truncated octahedron base cell has been selected as first experiment. Truncated octahedron is an Archimedean solid with cubic symmetry and it is constructed from a regular octahedron by the removal of six right square pyramids from each point. It has 14 faces (8 regular hexagonals and 6 squares), 36 edges and 24 vertices. The fracture morphology of the truncated-octahedron lattice structure turns out to be progressively collapse deformation and the tapered truncated-octahedron lattice is shear band dominated [15].

3D printing has been first described by Hull in 1986 [16]. In the concept the technology allows to manufacture objects by material addition with a reduced fraction of waste and with satisfactory geometric accuracy. Starting from a 3D computer model (CAD), many printing techniques have been employed to fabricate polymer components. The well-established techniques are fused deposition modeling (FDM), selective laser sintering (SLS) and stereolithography apparatus (SLA): each technique has peculiar advantages and limitations and the selection of the fabrication technique is function of the starting materials, processing speed, required resolution, costs and performance requirements of the final products. Dealing with polymer objects, FDM printers are the most commonly used ones thanks to the possibility of adoption of thermoplastics as PC, ABS and PLA with low melting temperature. FDM technique has been identified more suitable in this work for the manufacturing of PLA. In the FDM printer, filaments melt into a semi-liquid state in proximity of the nozzle and are extruded layer by layer onto the moving platform. In this way layers are fused together till the solidification in the final parts. By modifying the processing parameters such as layer thickness, printing orientation, raster width and angle it is possible to control the quality of the printed parts. On the other hands one disadvantage of FDM printers is that the useable material is limited to thermoplastic polymers with suitable melt viscosity. The melt viscosity should be high enough to provide structural support and low enough to permit

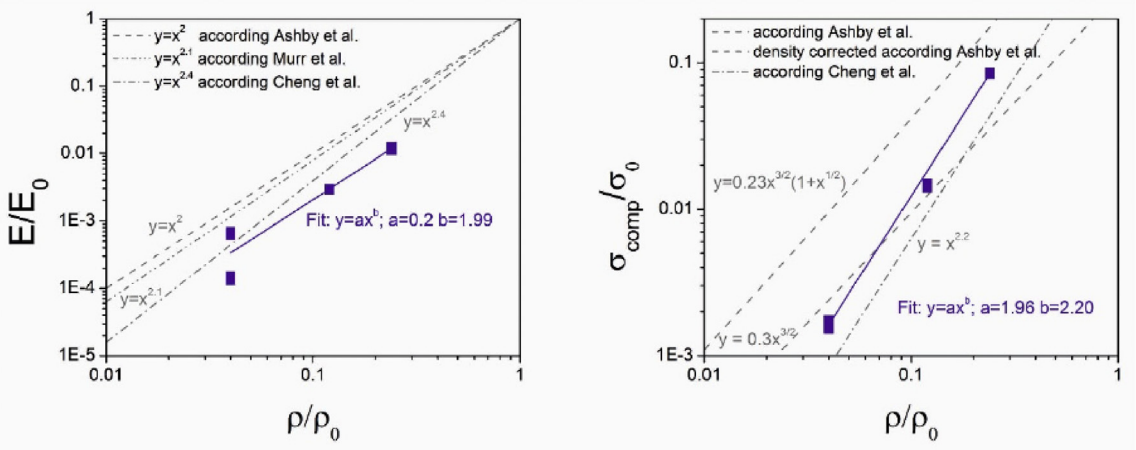

Fig. 1. Specific mechanical properties for the rhombi-dodecahedron sandwich structure vs specific density [12]. Models of Ashby, Murr and Cheng are compared in gray dotted lines.

extrusion. Another advantage is that FDM printing allows deposition of various materials simultaneously adopting multiple extrusion nozzles with different materials. Finally low cost, high speed and simplicity of the system complete the description [17].

2. Materials and experimental methods

For the above mentioned reasons the FDM technique has been identified suitable for the purpose of the research in terms of fixed and variable costs. The main goal of the paper doesn't concern the definition of a particular 3D printing process but rather the adoption of a suitable 3D printing technique in order to minimize the overall manufacturing costs for the production of a metal foams with open and preselected porosity. Poly lactic acid, a biodegradable polymer, has been selected as melting material. Environmental issues of global warming and plastic pollution have contributed to increase the demand of alternative materials. Biobased plastics are being developed to replace petroleum-based plastics due to the reduction of carbon emissions by the absorption of CO_2 from atmosphere by the bio-based raw materials. The production process of this bioplastic emits 68% less greenhouse gas than the production of common plastic. At the same time biodegradable plastics have been developed to reduce plastic pollution thanks to the faster degradation in comparison with traditional plastics. Poly lactic acid is one of the most successful bio-plastic among the rigid ones due to its good processability and mechanical properties. Its starting monomer can be easily derived 100% from renewable sources, for instance starch, sugar or beet through fermentation. PLA has mechanical strength, durability and transparency compared to other bio-degradable plastics and is widely employed for short lifetime packaging products such as foods. PLA can degrade promptly in a few months at a temperature of 58 °C [18]. The aerobic biodegradability can be evaluated, for instance, according to the standard ISO 14855−2:2018.

The technique presented in this paper is similar to the, so called, “lost-wax casting” with the main difference in the material used: the biodegradable polymer PLA instead of wax. The whole process is articulated in the following steps:

(1) −build-up of the model with 3D CAD;
(2) −export to CAM software for 3D printing;
(3) −3D printing of the model using PLA;
(4) −plaster casting on the PLA model;
(5) −mold drying;
(6) −PLA removing from the plaster;
(7) −metal casting into the plaster mold;
(8) −plaster removal to obtain a foam.

The build-up of the model has been made with 3D CAD, then it has been exported to CAM software for 3D printing with which to optimize the process parameters and the material (PLA) used. The first step consists in generating the elementary cell, truncated octahedron in this case (Fig. 2a). From its replication in the 3 space directions the cellular solid has been generated (Fig. 2b). The PLA model after 3D printing is reported in Fig. 2c. The selection of the characteristic parameters thickness (t) and edge cell (l) has been driven by the relative density to be obtained by the final foam. At the same time some printing parameters must be set, in particular: print speed (mm/s) and layer height (mm). After several attempts the optimum values of these parameters have been determined in 45 mm/s and 2 mm respectively in order to allow a good compromise between print quality, processing time and low cost.

After manufacturing of the model the successive step consists in the immersion of the model in a mixture of type 3 dental plaster and water (2:1 ratio). After that, the model has been left to dry in air for 45 min or, to accelerate the process, in oven at 100 °C for 15 min (Fig. 3a). The selected plaster has been type 3 dental one due to the excellent wettability and fluidity also in filling complex shapes.

After plaster solidification it is necessary to remove the PLA model. To do that a thermal treatment in the oven has been performed at 600 °C in order to burnout the PLA and leave clean the mold. Plaster mold without the PLA model inside after burnout of PLA is shown in Fig. 3b. The cells with hexagons squares can be easily distinguished (geometric figures that make up the truncated octahedron). At this point of the process it is possible to pour the molten commercially pure aluminum (99.9%) into the mold inside an oven set at 750 °C, temperature higher than the melting point of Al (660 °C). The final step consists in the removal of the plaster in an ultrasound bath so that the final aluminum foams (Fig. 3c) can be obtained. The last three manufacturing steps are illustrated in Fig. 3(a−c).

3. Results and discussion

In Fig. 2 b and c, respectively, cellular solid model and 3D model after 3D printing are evidenced. The printed model is well replicated in terms of porosity and morphology, with high accuracy and reduced surface roughness of the cell walls. Fig. 4 a reveals the morphology of the PLA model manufactured by means of FDM technique observed at the stereo microscope and with low

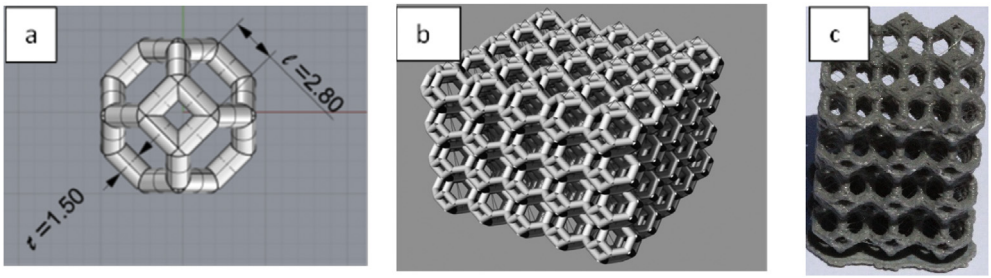

Fig. 2. (a) truncated octahedron elementary cell; (b) cellular solid; (c) 3D model after 3D printing.

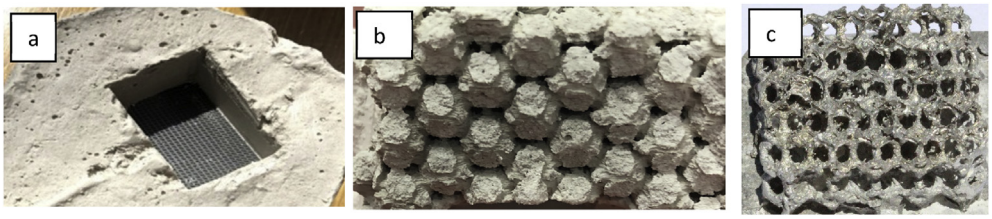

Fig. 3. (a) plaster mold with PLA model inside after solidification. – (b) plaster mold without PLA model inside after burnout of PLA. (c) Aluminum foam with open porosity after casting at the end of the process.

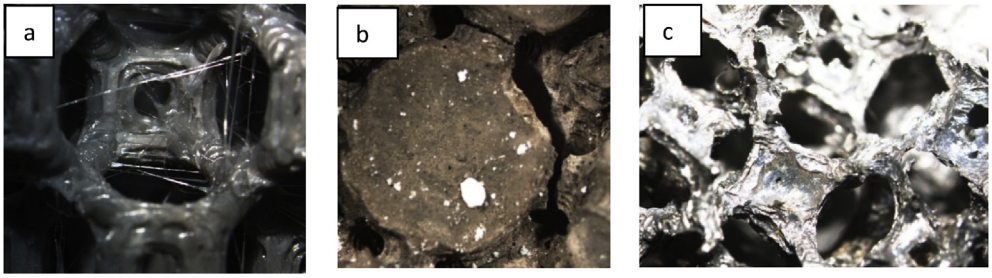

Fig. 4. Optical observations at the stereo microscope. (a) Detail of the PLA model. (b) plaster mold. (c) aluminum foam.

magnification factor (10X). It is evident the truncated octahedron shape of the poly lactic acid open cell foam. Also the characteristic thickness (t) and edge cell (l) measured are strictly correlated to the designed ones, that are 1.5 and 2.8 mm respectively. Measured values are within ± 10% tolerance range with the designed ones, taking into account the spatial resolution of the 3D printer according to the selected parameters (print speed and layer height). Better accuracy in the replication process can be achieved with the drawback of longer processing times and lower layer height. The obtained Al foam structure and the starting one made of PLA are the same thanks to the replication method illustrated in this work. The manufactured foam has a homogeneous structure with open pores which replicates the original PLA model. More in general the morphology and porosity size can be easily customized by selecting a different model and replicating it in Al foam. Many cell types can be manufactured and, as a consequence, also density and related mechanical properties. In the PLA model the layers, function of the layer height parameter, are thin and regular (Fig. 4a), therefore there is no presence of the defect defined “shifted layer”. This means that the extruder speed has been correct. One of the most common defects in printing for FDM, namely “stringing” (Fig. 4a), are unwanted plastic strings between the parts of the object. The geometry of the pre-selected cell was acceptable and almost free from defects. The whole structure of the selected foam (hexagons and squares, see Fig. 4c) is in good agreement with the pre-selected geometry in the PLA starting model. Moreover the moderate stringing defect in the model doesn't lead to defects in the plaster mold. As can be observed in Fig. 4b no presence of strings inside the plaster mold is evidenced. However, the cell thicknesses and edges in the metal foams are sufficiently homogeneous along the structure. After filling with liquid plaster, the negative shape of the model is obtained. A detail of the plaster mold is illustrated in Fig. 4b after the burnout of the PLA, as evidenced by the dark aspect of the surface. Finally, after casting, the open cell Al foams manufactured with the novel method is illustrated in Fig. 4c, replicating the structure of the starting model and the PLA foam.

Further work is needed in order to increase the quality of the porosity roughness and wall thickness of metal foams, comparing the benefits of higher pressure applied to the liquid Al, for example as in pressure-assisted solidification technique. Also the adoption of typical casting Al–Si alloys, instead of pure Al, needs to be investigated in order to reduce melting temperature and melt viscosity and at the same time increase overall mechanical properties.

4. Conclusions

This work aims to present an innovative and alternative process to obtain open porosity foams with a good repeatability in terms of pre-selected cell shape and size. The main advantages of this technique are listed in the following:

(1) flexibility of the production process as it starts from the design of the elementary cell, in terms of thickness and length of the sides of the prism, identified according to the final application.

The selected parameters can be determined in such a way as to adapt the lost PLA process to the generation of open-porosity aluminum foams. FDM 3D printing technique of PLA material has been adopted. By way of example, truncated octahedron elementary cell has been manufactured, with a thickness cell $t = 1.5$ mm and length cell $l = 2.8$ mm;

(2) reduced manufacturing cost;
(3) reduced processing time;
(4) bio-degradable plastic adoption (PLA) for the sacrifice and replication process.

All these points are important features of the presented method. Printer setup has been selected for speed at 45 mm/s and for layer height at 2 mm. PLA foams have been filled with liquid type 3 dental plaster to obtain a mold and solidified. Then, the PLA has been removed at 600 °C allowing its burnout. After that molten Al has been poured in the plaster mold in an oven at 750 °C. After Al solidification the plaster can be easily removed in an ultrasonic bath so that an open cell porosity foam can be obtained. The geometry selected with CAD model has been accurately replicated by 3D printing with FDM technique and appears almost free from defects. The Al foam structure shows hexagons and squares. The moderate stringing defect in the model doesn't lead to defects in the plaster mold and in the final foam. However, the cell thicknesses and edges in the metal foams are sufficiently homogeneous along the structure. Further efforts must be spent to optimize the process parameters in Al casting, for instance by the adoption of pressure-assisted solidification technique and the utilization of Al–Si casting alloys.

Author contributions

Authors declare equal contributions to this work.

Conflicts of interest

The authors declare that there is no conflicts of interest.

References

[1] Y. Bienvenu, Application and future of solid foams, C.R. Phys. 15 (2014) 719–730, https://doi.org/10.1016/j.crhy.2014.09.006.
[2] D. Bhate, C.A. Penick, L.A. Ferry, C. Lee, Classification and selection of cellular materials in mechanical design: engineering and biomimetic approaches, Designs 3 (1) (2019), 19, https://doi.org/10.3390/designs3010019.
[3] J. Banhart, Manufacture, characterization and application of cellular metals and metal foams, Prog. Mater. Sci. 46 (6) (2001) 559–632, https://doi.org/10.1016/S0079-6425(00)00002-5.
[4] G. Costanza, G. Gusmano, R. Montanari, M.E. Tata, Manufacturing routes and applications of metal foams, Met. It. 95 (2) (2003) 31–35.
[5] G. Costanza, R. Montanari, M.E. Tata, Optimization of TiH2 and SiC content in Al foams, Met. It. 97 (6) (2005) 41–47.
[6] G. Costanza, G. Gusmano, R. Montanari, M.E. Tata, N. Ucciardello, Effect of powder mix composition on Al foam morphology, P. I, Mech. Eng. L- J. Mat. 222 (2) (2008) 131–140.
[7] G. Costanza, F. Mantineo, S. Missori, A. Sili, M.E. Tata, Characterization of the compressive behaviour of an Al foam by X-ray computerized tomography, TMS Light Metals (2012) 533–536.
[8] G. Costanza, G. Dodbiba, M.E. Tata, Optimization of the process parameters for the manufacturing of open-cells iron foams with high energy absorption, Proc. Struct. Int. 2 (2016) 2277–2282, https://doi.org/10.1016/j.prostr.2016.06.285.
[9] G. Costanza, M.E. Tata, Parameters affecting energy absorption in metal foams, Mat. Sci. For. 941 (2018) 1552–1557, https://doi.org/10.4028/www.scientific.net/MSF.941.1552.
[10] G. Costanza, M.E. Tata, Recycling of Exhaust Batteries in Lead-foam Electrodes, TMS Annual Meeting and Exhibition, 2013, pp. 272–278.
[11] L.J. Gibson, M.F. Ashby, Cellular Solids. Structure and Properties, 2nd ed., Cambridge University Press, Cambridge, 1997.
[12] K.G. Prashanth, L. Löber, H. Klauss, U. Kühn, J. Eckert, Characterization of 316L steel cellular dodecahedron structures produced by selective laser melting, Technologies 4 (2016), 34, https://doi.org/10.3390/technologies4040034.
[13] L.E. Murr, K.N. Amato, S.J. Li, Y.X. Tian, X.Y. Cheng, S.M. Gaytan, E. Martinez, P.W. Shindo, F. Medina, R.B. Wicker, Microstructure and mechanical properties of open-cell biomaterials prototypes for total knee replacement implants fabricated by electron beam melting, J. Mech. Behav. Biomed. Mater. 4 (2011) 1396–1411, https://doi.org/10.1016/j.jmbbm.2011.05.010.
[14] X.Y. Cheng, S.J. Li, L.E. Murr, Z.B. Zhang, Y.L. Hao, R. Yang, F. Medina, R.B. Wicker, Compression deformation behavior of Ti-6Al-4V alloy with cellular structures fabricated by electron beam melting, J. Mech. Behav. Biomed. Mater. 16 (2012) 153–162, https://doi.org/10.1016/j.jmbbm.2012.10.005.
[15] D. Qi, H. Yu, M. Liu, H. Huang, S. Xu, Y. Xia, G. Qian, W. Wu, Mechanical behaviors of SLM additive manufactured octet-truss and truncated-hoctaedron lattice structures with uniform and taper beams, Int. J. Mech. Sci. 163 (2019), 105091, https://doi.org/10.1016/j.ijmecsci.2019.105091.
[16] C.W. Hull, Apparatus for Production of Three-Dimensional Objects by Stereolithography, 1986. US patent 4575330A.
[17] X. Wang, M. Jang, Z. Zhou, J. Gou, D. Hui, 3D printing of polymer matrix composites: a review and prospective, Compos. Part B-Eng. 110 (1) (2017) 442–458.
[18] K.J. Jem, B. Tan, The development and challenges of poly (lactic acid) and poly (glycolic acid), Adv. Ind. Eng. Pol. Res. 3 (2) (2020) 60–70, https://doi.org/10.1016/j.aiepr.2020.01.002.